

RECEIVED BY OSTI

APR 29 1985

CONF-850410--31

THE EXPERIMENTAL BREEDER REACTOR II INHERENT SHUTDOWN
AND HEAT REMOVAL TESTS - TEST RESULTS AND ANALYSIS*.

CONF-850410--31

DE85 010483

H. P. Planchon, R. M. Singer, D. Mohr, E. E. Feldman,
L. K. Chang and P. R. Betten

EBR-II Division
Argonne National Laboratory
Argonne, Illinois 60439

The submitted manuscript has been authored
by a contractor of the U.S. Government
under contract No. W-31-109-ENG-38.
Accordingly, the U.S. Government retains a
nonexclusive, royalty-free license to publish
or reproduce the published form of this
contribution, or allow others to do so, for
U.S. Government purposes.

International Topical Meeting
on
Fast Reactor Safety
April 21-25, 1985
Knoxville, Tennessee

This report was prepared as an account of work sponsored by an agency of the United States Government. Neither the United States Government nor any agency thereof, nor any of their employees, makes any warranty, express or implied, or assumes any legal liability or responsibility for the accuracy, completeness, or usefulness of any information, apparatus, product, or process disclosed, or represents that its use would not infringe privately owned rights. Reference herein to any specific commercial product, process, or service by trade name, trademark, manufacturer, or otherwise does not necessarily constitute or imply its endorsement, recommendation, or favoring by the United States Government or any agency thereof. The views and opinions of authors expressed herein do not necessarily state or reflect those of the United States Government or any agency thereof.

DISCLAIMER

*Work supported by the U. S. Department of Energy under contract
W-31-109-Eng-38.

MASTER

DISTRIBUTION OF THIS DOCUMENT IS UNLIMITED

7/19

THE EXPERIMENTAL BREEDER REACTOR II INHERENT SHUTDOWN AND
HEAT REMOVAL TESTS - TEST RESULTS AND ANALYSIS*

H. P. Planchon, R. M. Singer, D. Mohr, E. E. Feldman,
L. K. Chang and P. R. Betten

EBR-II Division
Argonne National Laboratory
Argonne, Illinois 60439

ABSTRACT

A test program is being conducted to demonstrate that a power producing Liquid Metal Reactor (LMR) can 1) passively remove shutdown heat by natural convection; 2) passively reduce power in response to a loss of reactor flow and 3) passively reduce power in response to a loss of the balance of plant heat sink. Measurements and pretest predictions confirm that natural convection is a reliable, predictable method of shutdown heat removal and suggest that safety related pumps or pony motors are not necessary for safe, shutdown heat removal in a LMR. Measurements from tests in which reactor flow and heat rejection to the balance of plant were perturbed show that reactivity feedbacks can passively control power and temperature. This data is a basis for additional tests including a complete loss-of-flow without scram and a complete loss of heat sink without scram.

INTRODUCTION

The essential control and protection of a nuclear plant is maintaining a proper balance between the heat generated in the reactor and the heat removal from the reactor. If this balance is maintained locally and globally then temperatures of reactor structures--notably the fuel cladding and the primary reactor boundary--will be maintained within their design limits.

*Work supported by the U. S. Department of Energy under contract
W-31-109-Eng-38.

2

Traditionally LMR plant designs have utilized a combination of passive features and active systems and components to maintain the balance between heat generation and removal. For example, routinely power control depends significantly on the (passive) negative power coefficient and (active) manual or automatic movement of control rods. The heat removal is normally adjusted to match heat generation by (actively) controlling the flowrate through the reactor and (actively) controlling the balance-of-plant heat sink. Flow is distributed (passively) within the reactor by fixed, engineered pressure drops of the various reactor internal components.

The balance between heat generation and heat removal during upsets to normal operation (which may occur as a result of random failures of the active or passive equipment or as a result of severe natural phenomena) is likewise traditionally maintained by a combination of passive design features and active systems. During their licensing hearings, CRBRP (1) categorized these features and systems in a way that can be generalized to apply generically to LMR's. The four features/systems necessary to maintain the balance between heat generation and heat removal were listed as: 1) the (active, automatic) reactor shutdown systems, 2) (active and passive, automatic) shutdown heat removal systems, 3) means to prevent inlet pipe rupture (passive prevention of loss of coolant, and 4) (passive) means to maintain individual subassembly heat generation and heat removal.

The high degree of reliability which is required for nuclear control and shutdown functions can be realized with either an active systems or a passive features; however, the methods for achieving reliability for each are significantly different. The passive features--using for example the passive prevention of loss of working fluid and passive means to maintain individual subassembly heat generation and heat removal--use the inherently stable, compatible characteristic of LMR fuel, primary coolant and coolant boundary operating in a low pressure fault tolerant system to attain high reliability. The actual realization of the high reliability depends heavily on (1) the quality of the design process and its supporting analytical and test data base and (2) the quality of the manufacturing and construction process. In contrast, a high degree of reliability in the active systems is gained with equipment redundancy diversity and independence of high quality equipment. Redundancy enables continued functioning of the equipment even with random

2

failures. Diversity protects against a large class of common cause failures and independence pretests redundant equipment from potential environmental challenges that could otherwise lead to common cause failures. It is generally accepted that redundant diverse independent protection/control system can provide a high degree of reliability. However, it is also becoming more evident that the number of different separated systems and components required for higher and higher reliabilities result in a very complex design that is difficult to construct and cumbersome to maintain and operate. It is therefore believed that there are significant benefits to achieving the balance between heat generation and heat removal by passive means thus reducing the number of required redundant diverse separated safety systems. A move toward passive control and safety systems could also provide a broader more easily understood technical basis for licensing LMRs.

In conclusion then LMR design, construction and operation can potentially be simplified by replacing active systems with passive features for maintaining the balance between power and flow. However, a substantial set of test data is required to show the feasibility of passive control and provide a basis for the design of passively control systems.

Test Program Objectives

EBR-II has been conducting dynamic testing program particularly directed toward passive decay heat removal in liquid-metal-cooled reactors for some 10 years.⁽²⁾ This testing experience as summarized by Singer et al⁽¹⁾ has contributed toward the acceptance of natural convection as a passive diverse backup to active decay heat removal systems. With the idea of extending the understanding of natural convection heat removal and the goal of exploring the possibilities of passive shutdown for reduced heat removal capability, the objectives of the current testing program have been established as follows:

- 1) Demonstrate passive decay heat removal following reactor shutdown (natural circulation)
- 2) Demonstrate passive reactor shutdown following a loss of forced circulation (loss-of-flow without scram)
- 3) Demonstrate a passive reactor shutdown following a loss of balance of plant heat sink (loss of heat sink without scram)
- 4) Provide data for validation of computer codes

4

Additionally in the planning analyzing and testing the most significant parameter are identified tested and modeled. The information is available for design and safety analysis. The test methods may be a basis for methodologies to be used in acceptance or surveillance testing of inherent safety features.

PLANT DESCRIPTION

EBR-II is a sodium cooled fast breeder reactor plant. It generates about 20 MW of electricity when operating at design power of 62.5 MW thermal. It is a pool type plant with the reactor, primary coolant pumps and intermediate heat exchange (IHX) immersed in some ft of sodium in the primary pool. The two single stage centrifugal pumps, when operated at a rated speed of 1075 rpm, produce 4500 gpm at 200 ft head. The pumps are driven over a range of speeds from about 20% to 100% by an induction motor powered from a variable speed motor generator set. As described by Chang and Mohr,⁽³⁾ the time for the pump to coastdown, to a stop, is dependent on how electrical power is disconnected from the motor-clutch-generator-pump motor the drive line. For a typical loss of all AC power the coastdown time to pump stop is about 1 minute. The pumps take a suction of sodium from the pool and discharge to the inner (mostly fueled drivers) and outer (blanket and reflector assemblies) plena of the reactor. The flow split between the plena has been fixed since early operation of EBR-II. The sodium flows through the reactor, mixes in a outlet small plenum (flow through time of sec) and travels through an elevated "Z pipe" to the intermediate heat exchanger (IHX). The reactor consists of 16 rows of assemblies. The inner 6 rows were fueled driver assemblies. The fueled length is 343 mm and the flat-to-flat dimension is 56.1 mm. Each fueled assembly contains 91 elements composed of metallic fuel contained in a stainless steel clad with a sodium bond. The assemblies are supported at the bottom by a diagrid structure. The reactivity feedback typically provide a power reactivity decrement of 30¢ from critical isothermal conditions to the rated power conditions. As described by Chang and Mohr⁽³⁾ this is attributable to expansion of driver fuel (about 25%), expansion of sodium and steel (about 50%), and control rod expansion (about 25%). Additional feedbacks due to expansion of the support grid and expansion of sodium and steel in the lower reflector roughly produce a 2% reduction in power for an inlet temperature increase of one degree Farenheight. The IHX is a counter flow tube-in-shell heat exchanger with the primary sodium on the tube side.

The IHX is located above the reactor (inlet of IHX about 18 ft above the inlet of the reactor) to support natural convection cooling. A safety grade electromagnetic pump, located in the "Z pipe", provides about 5% flow to remove heat following reactor shutdown. Two NaK-to-air shutdown coolers are designed to be direct, safety grade, heat removal paths from the primary pool to outside air and thus backup the normal shutdown heat removal path via the secondary loop to the steam generators and balance-of-plant. Circulating sodium, in the secondary loop, removes heat from the IHX and transports it to the steam generator system. The secondary sodium pump is an electromagnetic pump rated at gpm and typically, when the reactor plant is shut down, the pump voltage is reversed to retard natural circulation flow thus allowing control of the plant cooldown rate.

Power is controlled by manual or automatic positioning of a control rod. Primary flow can be controlled by manually varying the speed of the primary coolant pumps. Normally flow is kept constant during power operation and the coolant temperature rise across the reactor is allowed to vary with power level. The heat removal from the primary tank is controlled by manually or automatically varying the secondary flow rate to keep the primary tank temperature at a desired point. Protection againsts imbalances in heat generation and heat rejection caused by sudden failures of equipment is provided by redundant sets of control rods actuated by redundant strings of a reactor shutdown system.

EBR-II is well instrumented and during testing some 300 variables (including powers, flows, temperatures, pressures and equipment status) were lagged at 1/2 sec intervals by the computerized plant data aquisition system. The key data for the tests was provided by two, instrumented, in-core subassemblies. The first XX09, is a fueled assembly positioned in core at one of the higher power, hottest positions. The other assembly simulates a relatively low power blanket subassembly in which the thermal response is sluggish and interassembly heat transfer is relatively more important. In both instrumented assemblies the flow is measured by redundant magnetic flowmeters.

Detailed measurement of the sodium temperature field in XX09 and XX10 are made with thermocouples. Measurements are made 1) at the assembly inlet, 2) in a distribution across the bundle at the reactor midplane, 3) in a distribution across the bundle near the top of the fueled section, 4) approximately

5.4 in. (137.2 mm) above the top of the fueled section, and 5) near the exit of the fuel assembly. The design-basis and steady-state performance of XX10, the instrumented simulated blanket assembly, is described by Betten et al⁽⁴⁾ and a hardware description of both assemblies is given by Poloncsik et al.⁽⁵⁾

TEST PREPARATIONS

The first group of tests were conducted in June 1984. They included natural circulation tests, flow reduction tests and heat sink reduction tests. Table I lists the tests. The planning, safety review and operation procedure preparation prior to the tests was extensive. Safety analyses were conducted to determine the peak fuel driver temperatures and peak blanket temperatures for the limiting tests. The analysis predicted the peak fuel temperatures for all tests would remain within the established limits (the fuel-clad eutectic temperature) for an anticipated design basis event. This was true even though the tests simulated some highly improbable failure conditions. As shown in Table I, the tank temperature was lowered from the normal 700°F operating point for some tests to provide additional margin. The effects of the EBR-II design basis accidents were also analyzed. The reactor shutdown system was found to provide adequate protection for these events showed they occur during testing. These safety analysis were reviewed and approved by the Division, Laboratory and DOE safety groups.

The tests were sequenced in order of increasing severity. A final set of pretest analysis was completed for each test just prior to testing. This analysis included best estimate and maximum and minimum (considering uncertainties) predictions of the XX09 temperature and flows. Using these predictions a "quick look" analysis was completed following each test and an assessment was made as to whether it was safe to proceed to the next test.

The tests were conducted in strict observance of detailed, step-by-step procedures. The procedures were prepared by operations experts based on input from the experimenters.

NATURAL CIRCULATION TESTS FROM POWER

The purpose of this group of tests was to demonstrate and provide measurements of the transition to natural circulation cooling following a sudden loss of primary forced circulation (loss of electrical power to the

TABLE I. Target Test Conditions

Test	Initial Conditions			Test Initiation
	Power %	Pri. Flow %	Sec. Flow %	
1	SD/RF ¹	100	2	Trip pri. pump
2	SD ²	5	2	Trip aux pump
3	SD	100	9	Trip pri. pump
4	36	40	38	Scram, trip pri. pump, trip sec. pump at 12.5 sec
5	36	40	38	Scram, rundown pri. pump, trip sec. pump
6	36	40	38	Scram, trip pri. and sec. pumps
7	75	100	87	Scram, trip pri. pump, manual rundown sec. flow
8	SD	100	10	Trip pri. pump
9	75	75	75	Scram, trip pri. pump, manual rundown sec. flow
10	SD	100	~ 0.5	Trip pri. pump
11	100	100	100	Scram, trip pri. pump, manual rundown sec. flow
12	SD	100	~ 0.5	Trip pri. pump
13	75	100	87	Scram, trip pri. and sec. pumps
14	SD	100	10	Trip pri. pump
15	75	75	75	Scram, trip pri. pump, trip sec. pump
16	SD	75	10	Trip pri. pump
17	100	100	100	Scram, trip pri. and sec. pumps
18	SD	100	5	Trip pri. pump
19	25	25	~ 25	Ramp pri. flow to 30%, hold, return
20	25	25	25	Raise tank temp., hold, return
21	25	25	25	Ramp pri. flow to 30%, hold, return with power with control rods
22	25	25	25	Ramp tank temp., hold, return power with control rods
23	50	50	50	Ramp flow to 62.5%, hold, return
24	50	50	50	Ramp tank temp., hold, return
25	70	70	70	Ramp flow to 90%, hold, return
26	70	70	70	Ramp tank temp., hold, return

¹Conducted after lengthy shutdown.²Shutdown.

main coolant pumps and auxiliary pump) while at power. Nine tests of this type were conducted. All of these tests were initiated by tripping the main coolant pumps and scrambling the reactor. The parameters that were varied from test to test were the initial power and initial flow conditions, and the mode of operation of the secondary loop pump.

The most severe test (SHRT 17) involved a simultaneous loss of electrical power to the main coolant pumps, the auxiliary pump, and the secondary loop pump, and a reactor scram from 100% power and flow.

Thus the test simulated a limiting loss of heat removal from the reactor followed by totally passive (natural circulation) decay heat removal from the reactor. Figure 1 shows temperatures (predicted and measured) indicative of the response of EBR-II to the SHRT 17 loss of forced circulation. Both the pretest predictions and the measured temperatures correspond to coolant temperature at the top of the active core. The predictions were made with the NATDEMO and HOTCHAN codes prior to conducting the test. The maximum, nominal and minimum curves which are labeled "MAX", "NOM", and "MIN", respectively, are respectively the HOTCHAN predictions for XX09 with positive uncertainties, without uncertainties and will negative uncertainties. The temperature measurements shown in Fig. 1 are raw data from TTC 31 (the hottest thermocouple) and were taken during testing for monitoring purposes. It should be noted that TTC 31 is one of 13 "top-of-core" (coolant) thermocouples which are all located 0.83 in. below the actual top of fuel. However, because of other compensating effects (i.e., offset of $\sim +8^{\circ}\text{F}$ and center of bundle location), the TTC 31 readings can be directly compared with the true top-of-core predictions without introducing significant error.

Trends in the test data, are consistent with previous thought and indicate that the most important parameters determining the peak fuel temperatures during a transition to natural circulation are 1) the heat generation rate (decay power), 2) the abruptness with which the heat removal rate changes (flow coastdown rate), 3) heat transfer and flow redistributions within the reactor, and 4) the natural heads and pressure drops at low flow conditions. The post scram decay power used in the pretest predictions are based on Shure's⁽⁷⁾ correlation and an estimated power history. For most of the tests no attempt to control the pretest power history was made; so, a conservatively long time at power prior to the tests was assumed. Thus the decay power level

was overestimated in the pretest predictions. For SHRT 17, the pretest predictions were updated the day before the test with a projected power history that was later realized. The more realistic power history resulted in a more accurate decay power and contributed to the good agreement between pretest predictions and measurements shown in Fig. 1.

The pump coastdown dynamics were based on extensive testing of the pumps. The pump/flow coastdown rate used in the tests and analysis simulates the coastdown following a loss of AC power to the pump/pump drive system. It is referred to as a mode trip in ref. 3 and its characteristics had been established by extensive testing.

The NATDEMO-HOTCHAN pretest predictions shown in Fig. 1 include effects of inter/intra assembly heat transfer and flow redistribution in flattening the temperature profiles within XX09 and between XX09 and cooler assemblies. A detailed analysis of the data which will quantify the contribution of each of these phenomena on reducing peak temperatures have not been completed. However, an order of magnitude estimate of the overall reduction of peak temperature due to the combined effects can be made by comparing the ratio of maximum to initial power to flow ratio to the ratio of maximum to initial temperature rise in XX09 (inlet to the hottest measured point). This comparison shows the maximum to initial ratio of temperature rise is less than half the ratio of maximum to initial power to flow ratio suggesting at least a factor of two reduction in peak temperature.

The transient development of the primary loop natural head through the driver region is shown in Fig. 2. Head changes are shown for the reactor, the "Z pipe" (between reactor and IHX), the IHX and the path from the IHX to the reactor inlet. This figure in conjunction with Fig. 1 is helpful in understanding the dynamics of the transition to natural circulation. The test was initiated by a reactor scram and pump trip. Initially the core is cooled nearly to inlet temperature (Fig. 1) and the pipe between the reactor and IHX is filled with cooler sodium. The cooler sodium causes the initial decrease in the natural head of the reactor and "Z pipe". As the pump slows down and stops (at about 50 sec) forced flow decreases, the decay power heats the channel sodium and the reactor head begins to recover. The head in the IHX also starts to increase. (Initially the IHX head decreases, apparently because the secondary flow coasts down faster than the primary flow resulting in

temporary undercooling of the primary sodium in the IHX.) The steady increase of IHX head shown in Fig. 2 is caused by 1) cooler primary sodium (stored in the "Z pipe" immediately following the scram) spilling into the down flowing primary side of the IHX and 2) the effectiveness of the secondary flow in removing heat in the IHX. The secondary flow is significantly larger than primary flow tending to move the active heat transfer region in the IHX to the upper tube sheet, decreasing the average sodium density in the primary side of the IHX, and increasing the overall primary natural convection driving head. As the heads recover, flow through XX09 increases and the temperature peaks. At times beyond the temperature peak, a quasi-equilibrium is approached in which the gradually decreasing rate of heat generation in the core is almost matched by a gradually decreasing rate of heat removal by the coolant. this is indicated by the decreasing flow and temperature in the XX09 subassembly.

As shown in Fig. 2 these are large changes in thermal driving head occurring in the IHX and in the flow circuit between the reactor and IHX. The figure underscores the importance of the layout and dynamics of plant components to natural convection performance. As shown in Fig. 1 there is excellent agreement between the predicted and the raw, measured data. Further examination are necessary but these results and the analysis presented in Ref. 6 further confirm that passive decay heat removal can be accomplished in a reliable predictable manner by natural circulation. The results when taken with the successful results of the FFTF⁽⁸⁾ tests suggest that natural circulation could be used in future LMR plants as a primary means of safety related decay heat removal and thus active safety related equipment such as pony motors and their supporting power supplies and instrumentation are not required.

NATURAL CIRCULATION TESTS FROM SHUTDOWN CONDITIONS

As shown in Table I nine natural circulation tests were conducted from shutdown conditions. Most of the tests (tests 3, 8, 10, 12, 14, and 16) were conducted after running the primary coolant pumps at high flow for a few minutes to attain an isothermal condition and then initiating the test by tripping both the main coolant pumps and the auxiliary pump. the ensuing transient is characterized by 1) a gradual flow coastdown to nearly zero flow, 2) heating and development of thermal heads in the reactor and 3) developed of flow. The temperature rise in these transients was found to be mild.

The SHRT 1 and SHRT 2 tests were most unique tests in this group. SHRT 1 was conducted at the end of a 1 month maintenance shutdown shortly after the instrumented subassemblies XX09 and XX10 were installed and prior to their irradiation. The test was initiated by tripping the main coolant pumps from a fuel flow, nearly isothermal condition. Because XX09 and XX10 were not irradiated interassembly heat transfer is believed to be a significant contributor to the slow measured temperature rise. To contrast the effects of internal heat source, a similar test is planned after a year of irradiation of XX09 and XX10 when the power generation is about twice the unirradiated power level.

The SHRT 2 test was initiated from a steady state, hot standby condition with the auxiliary pump providing about 5% flow (main coolant pumps off). The transient was initiated by deenergizing the auxiliary pump. This resulted in a sudden flow reduction. The temperatures in the reactor increase sharply, as shown in Fig. 3, and establish sufficient head and flow to carry away the decay power. As shown in the figure there is a good agreement between the pretest predictions and measure peak temperatures. After the temperature peak the agreement is not as good. This may be due to the pressure drop in XX09 being slightly larger at very low flow (0.5 gpm) than expected. This is consistent with measurements of flow in XX09 although it is difficult to confirm because of the flow measuring inaccuracies in the XX09 flowmeters of low flow. Further post test analysis is considering uncertainties in decay power as well as flow may resolve some of this uncertainty.

In conclusion, the data from the natural circulation tests from shutdown conditions confirm that these transients are generally less severe than natural circulation transients from high power. Agreement between predicted and measured peak temperatures is good. These transients frequently involve a low flow, and a small temperature rise. In this case there is a larger uncertainty in the calculations and measurements. However, the larger uncertainties are to tolerance because there is a corresponding larger margin to temperature limits.

FLOW PERTURBATION TESTS

Four flow perturbation tests were conducted in the June 1984 test window. The tests were designed to 1) demonstrate the inherent response to flow changes that could occur during normal load changes of an LMR and 2) Identify

and quantify the reactivity feedback coefficients that govern the power response for an unscrammed loss-of-flow. The tests were initiated from steady-state conditions of 25%, 50% and 70% power and flow as shown in Table I (see tests 19, 21, 23, 25). The flow was perturbed ramping primary pump speed to 120 to 130% of its initial value. The sodium temperature at the reactor inlet was maintained as constant as possible by varying secondary flow and thus controlling the heat rejection via the IHX. In all the tests reactor temperatures and power were allowed to freely respond to the flow perturbation. After a steady state evolving in tests 19, 23, and 25 the flow was quickly returned to its initial value. In test 21 a calibrated control rod was positioned to return power to its initial value thus obtaining a measure of the reactivity introduced by the flow perturbation.

Representative raw data for the test conducted from 70% power and flow (SHRT 25) are shown in Figs. 4 through 7. The figures were generated by the EBR-II plant data acquisition system (DAS) as the tests were being run and were used to monitor the progress of the tests. Figure 4 shows the measured core flow through the instrumented subassembly XX09. Figure 4 shows a representative in-core temperature response as measured on TTC 31. The excess reactivity, calculated online by the EBR-II plant DAS is shown in Fig. 6, and the measured power response is shown in Fig. 7. The data indicate that the reactivity feedbacks tend to adjust power in response to flow perturbations thus tending to maintain the balance between heat generation and heat removal and core temperatures within the operating range. Figure 8 gives further insight into the reactivity feedback mechanisms governing this process. The figure shows normalization values of measured flow power and temperature and calculated reactivity for the first part of the transient. The flow and temperature rise (ΔT) are XX09 measurements. The power was measured with the plant nuclear instrumentation. The power to flow ratio (P/F) was simply the ratio of measured power and flow.

All these quantities are ratioed to their initial value. The reactivity was calculated by NATDEMO in post test analysis. It was scaled and added to 1.0 for easy comparison to the other quantities. Comparing the P/F and ΔT ratios shows that the fuel region responds very quickly to the flow perturbation. For flow perturbations, the EBR-II reactivity feedback are dominated by mechanisms proportional to the sodium ΔT or the power to flow ratio (core and

upper reflector sodium and steel expansion, control rod drive line expansion and to some extent fuel expansion); therefore, one would expect the reactivity to vary roughly as the ΔT and P/F ratio. As shown in the figure, this is the case. It then follows that the lag between the driver flow and the responding power is almost totally to time lags in the nuclear kinetics specifically the delayed neutrons.

The relative size of the various components of feedback for the flow increase is shown in Fig. 9. As shown, significant feedbacks tending to raise power and keep the ΔT constant come from the sodium and metal expansion in the core and reflector and the control rod drive line expansion. The fuel terms, due to expansion and Doppler, initially contribute positive reactivity because of general cooling; however, as the power in the fuel increases the fuel temperature increases and the fuel reactivity feedback. The bowing reactivity as shown is negative throughout the transient. The relative size of the bowing reactivity shown in the figure is conservatively overstated by about 25%. As discussed by Chang and Mohr, the bowing reactivity is proportional to power to flow ratio. The equilibrium power is determined by the balance of the positive feedbacks from reactivity terms proportional to P/F and the negative feedback from the reactivity terms proportional to power (fuel expansion and Doppler). As shown in Fig. 5 the power equilibrium (about 25% above the initial value) is close to the flow perturbation (about 30% above the initial value). This is true in EBR-II because the fuel reactivity feedback coefficients are small and the ΔT from the metallic fuel to sodium which is (proportional to power) is relatively small compared to the coolant ΔT (which is proportional to P/F). Consequently, the total reactivity change that is a function of power alone is relatively small particularly when compared to an oxide fueled core. As a result of the dominance of the reactivity feedbacks that are a function of P/F, the power closely follows flow perturbations.

In summary the results of the flow perturbation tests show that EBR-II responds stability and predictability to flow perturbations tending to keep the power to flow ratio and the sodium temperature increase across the core nearly constant. This behavior suggests that passive mechanisms could be used for plant control. The data from these tests were used as discussed in ref. 3 to validate models and show that loss of flow without scram tests could be safely conducted in EBR-II.

14 HEAT SINK PERTURBATION TESTS

Four heat sink perturbation tests were conducted in the June 1984 test window. The tests were designed to 1) demonstrate the inherent response to changes in heat rejection to the balance of plant that could occur during normal load changes of an LMR and 2) identify and quantify reactivity feedback coefficients that govern the power temperature for a complete loss of the balance of plant heat sink without scram.

The heat sink perturbation tests, similar to the flow perturbation tests, were initiated from 25%, 50% and 70% power as shown in Table I (see tests 20, 22, 24 and 26). In all these tests the measured reactor inlet temperature was controlled by manually varying the secondary loop flow and hence varying the heat rejection rate from the primary tank via the IHX. The idealized goal in tests 20, 24 and 26 was to rapidly increase the reactor inlet temperature by about 20°F, hold the temperature until a plant wide steady-state evolved and then return the temperature to its original value. In test 22 a calibrated control rod was used to return reactor power to its initial value. In all of the tests, the primary loop flow was held constant. The reactor power and temperatures were allowed to respond freely to the inlet temperature perturbations.

The heat sink perturbations were simulated by varying secondary flow for two reasons as follows: 1) the test represents a wide range of balance of plant transients including reduction of coolant flow in the secondary and loss of feedwater upsets in the steam plant and 2) the test could be run easily and without risk of damaging the plant equipment.

Representative data for the test run from 70% power (SHRT 26) are shown in Figs. 9 through 12. The reactor inlet temperature was perturbed by manually changing the secondary loop flow as shown in Fig. 9 while primary flow was held fixed. The perturbations in secondary loop flow altered the IHX heat rejection resulting in a change in IHX primary outlet temperature and consequent change in reactor inlet temperature. The inlet temperature response is shown in Fig. 10. Reactor inlet temperature variation causes the reactor power to change (Fig. 11) due to reactivity feedback, and consequently affects temperature in the reactor. Figure 12 gives the measured XX09 temperature reading from TTC 31. Note that the increase in inlet temperature causes a significant decrease in power and core outlet temperature. The

steady-state power and reactor outlet temperature that results from the inlet temperature perturbation is governed by the size of the temperature coefficient of reactivity at the reactor inlet as compared to the temperature coefficient in and above the reactor. The negative temperature coefficient of reactivity in the core inlet region is provided by expansion of the upper grid supporting the core and by sodium and steel expansion in the lower reflector. The total reactivity feedback from the inlet region practically, dependent on inlet temperature changes and is independent of power. The principal contributors to reactivity feedback in the remainder of the reactor are bowing and the thermal expansion of fuel, steel sodium and the control rod drive lines as previously discussed. With constant flow the core feedbacks are a function of the temperature increase at the inlet and temperature decreases due to power reductions. The resulting steady-state power is fixed by the balance of the inlet region reactivity change (negative for temperature increases) and the core region reactivity change (positive for a power reduction) so that for a large temperature coefficient of reactivity, as is the case for EBR-II, a 20°F increase in inlet temperature results in approximately a 100°F temperature decrease in XX09.

In summary the data from the heat sink perturbation tests show that EBR-II inherently adjusts power to accommodate increases or decreases of the heat sink. The data suggest a characteristic that could possibly be used in a passive control mode. The data from the tests show the predictions in ref. 9 are conservative and verify that tests of a loss of heat sink without scram can be safely conducted in EBR-II.

SUMMARY AND CONCLUSIONS

The data from the first groups of tests indicate the viability of passive means of removing decay heat and reducing power in response to reduce flow or reduce heat rejection from the reactor. The measurements of peak temperatures from the natural circulation tests agreed well with the pretest predictions. This is consistent with similar good agreements between natural circulation predictions and tests that have previously been observed on both EBR-II and FFTF. The good agreement and the mildness of the natural circulation transient suggest that natural circulation could confidently be relied upon to the primary means of decay heat removal in future LMR designs, and that safety re-

lated pony motors, auxiliary pumps and their associated power supplies, instrumentation and control need not be safety related.

The data from the flow perturbation tests and from the heat sink perturbation tests show that reactor feedback mechanisms act to reduce power for both types of reduced heat removal situations. For a flow perturbation the reactor feedback keeps the power to flow ratio nearly constant. For an inlet temperature increase the outlet temperature never exceeds its initial value. The data from both tests suggest that part of the overall control of an LMR could rely on passive response of the plant. The data from the tests have been used to show that tests of loss of flow without scram and loss of heat sink without scram can be safely conducted in EBR-II.

REFERENCES

1. Applicants testimony concerning whether HCDA's should be DBA's, Exhibit 87 in the matter of USDOE, Project Management Corp., and TVA (Clinch River Breeder Reactor Plant Docket 50-537) before the USNRC Atomic Safety and Licensing Board, July 5, 1983.
2. R. M. Singer et al., "Decay Heat Removal and Dynamic Plant Testing at EBR-II," Proceeding of Second Specialists' Meeting on Decay Heat Removal and Natural Convection in LMFBR's, Brookhaven National Laboratory (April 1985).
3. L. K. Chang and D. Mohr, "The Effect of Primary Pump Coastdown Characteristic, on Unprotected Loss-of-Flow Transients in EBR-II," Proceedings of Second Specialists' Meeting on Decay Heat Removal and Natural Convection in LMFBR's, Brookhaven National Laboratory (April 1985).
4. P. R. Betten et al., "Concept and Design Basis and Temperature Predictions in a Simulated Instrumented LMFBR Blanket Subassembly," to be presented at the Third Int'l. Meeting on Reactor Thermal-Hydraulics, Newport, Rhode Island, October 1985.
5. J. Poloncsik et al., "The Experimental Breeder Reactor (EBR-II) Instrumented Subassemblies, INSAT XX09 and INSAT XX10," Amer. Nucl. Soc., Proc. Fast, Thermal and Fusion Reactor Experiments, Salt Lake City, Utah, Vol. 1, pp. 1-276 to 1-287, April 12-15, 1982.

6. E. E. Feldman, D. Mohr, L. K. Chang, P. R. Betten, H. P. Planchon, and J. F. Koenig, "Protected Loss of Primary and Secondary Pumping Power in the EBR-II," presented at this meeting.
7. K. Shure, "U²³⁵ Fission Product Decay Energy--1972 Reevaluation," USAEC Report WAPD-TM-1119, Westinghouse Electric Corp., NTIS, 1972.
8. A. Cheung, R. D. Coffield, K. Daschke, R. Markley, H. P. Planchon, W. J. Severson, Y. S. Tang, "Predictions of Natural Circulation Tests in FFTF," ASME Technical Paper 82-NE-25.
9. E. E. Feldman and D. Mohr, "Unprotected Loss-of-Heat Sink Simulation in the EBR-II Plant," ASME Technical Paper 84-WA/HT-7.

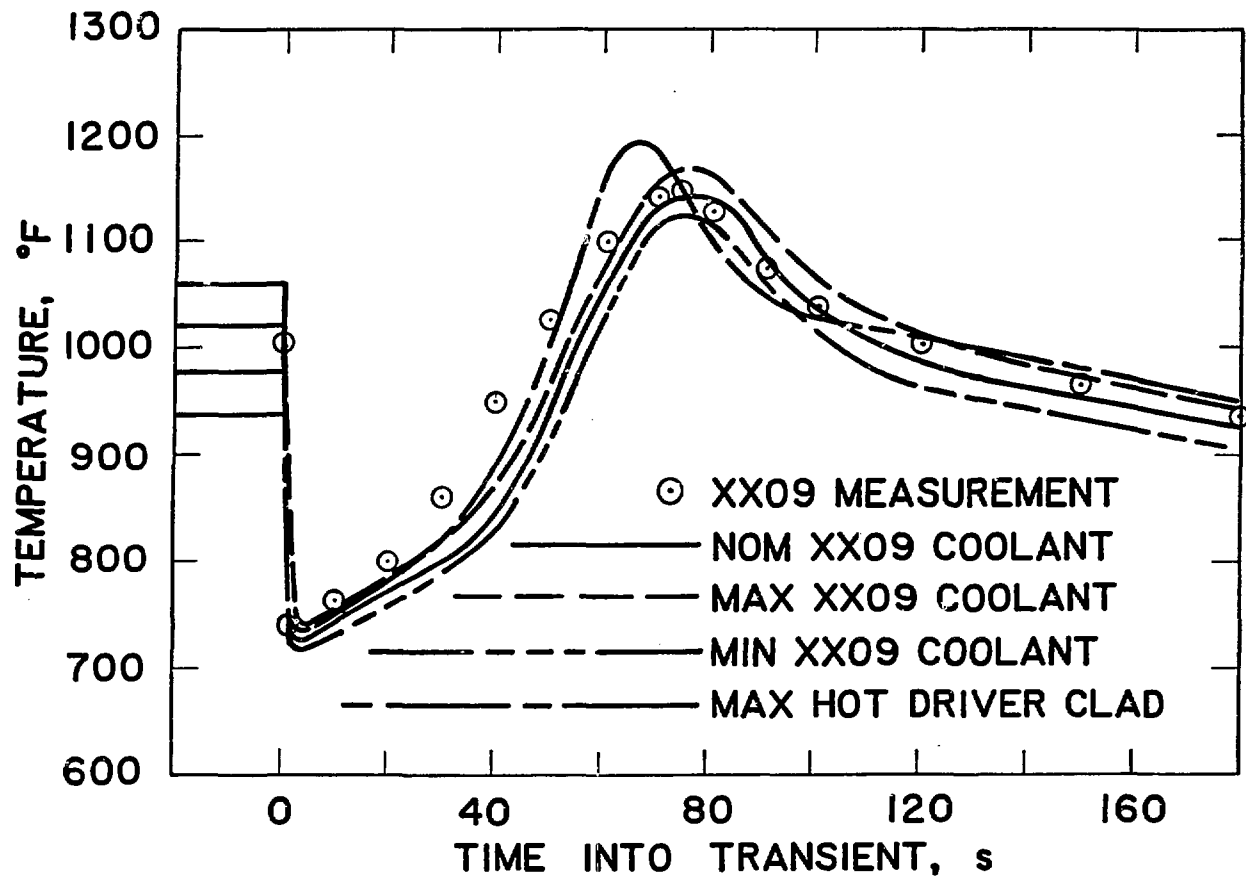


Fig. VI.10

Fig. 1. Measured and Predicted Top of Core Temperatures for the Transition to Natural Circulation from Full Power (SHRT 17)

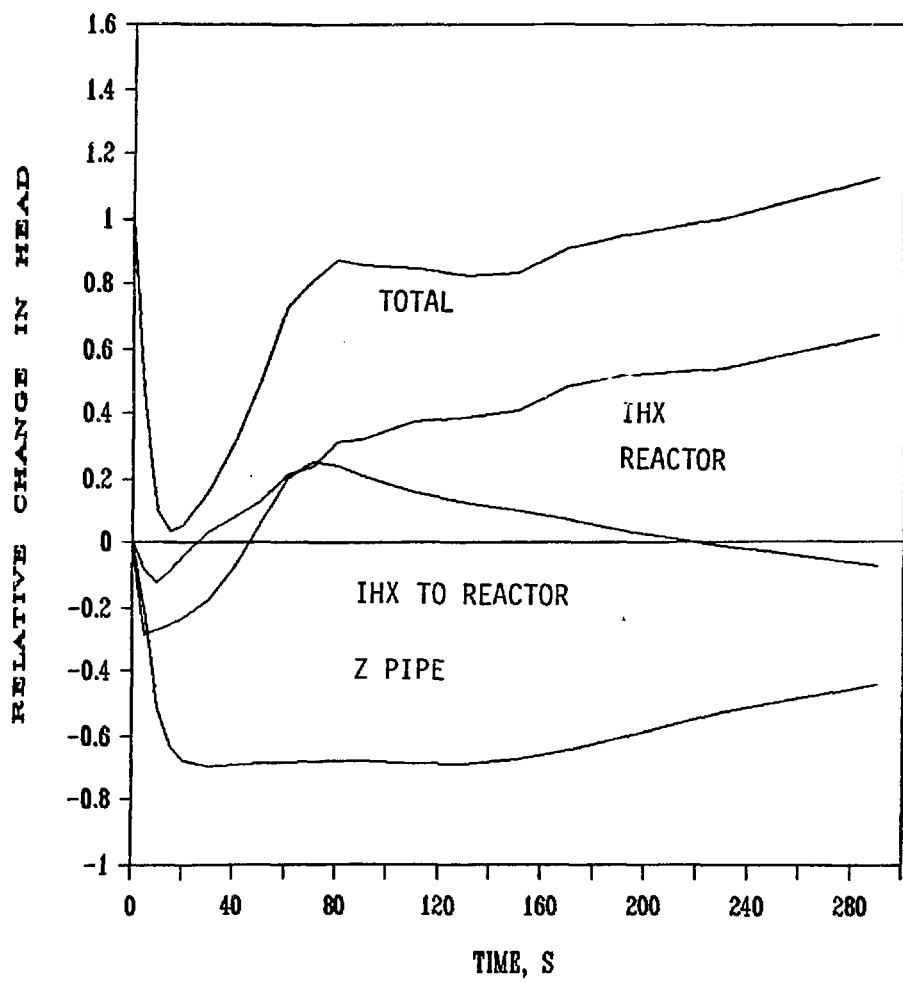


Fig. 2. Change in Natural Heads in the Primary Circuit for SHRT 17

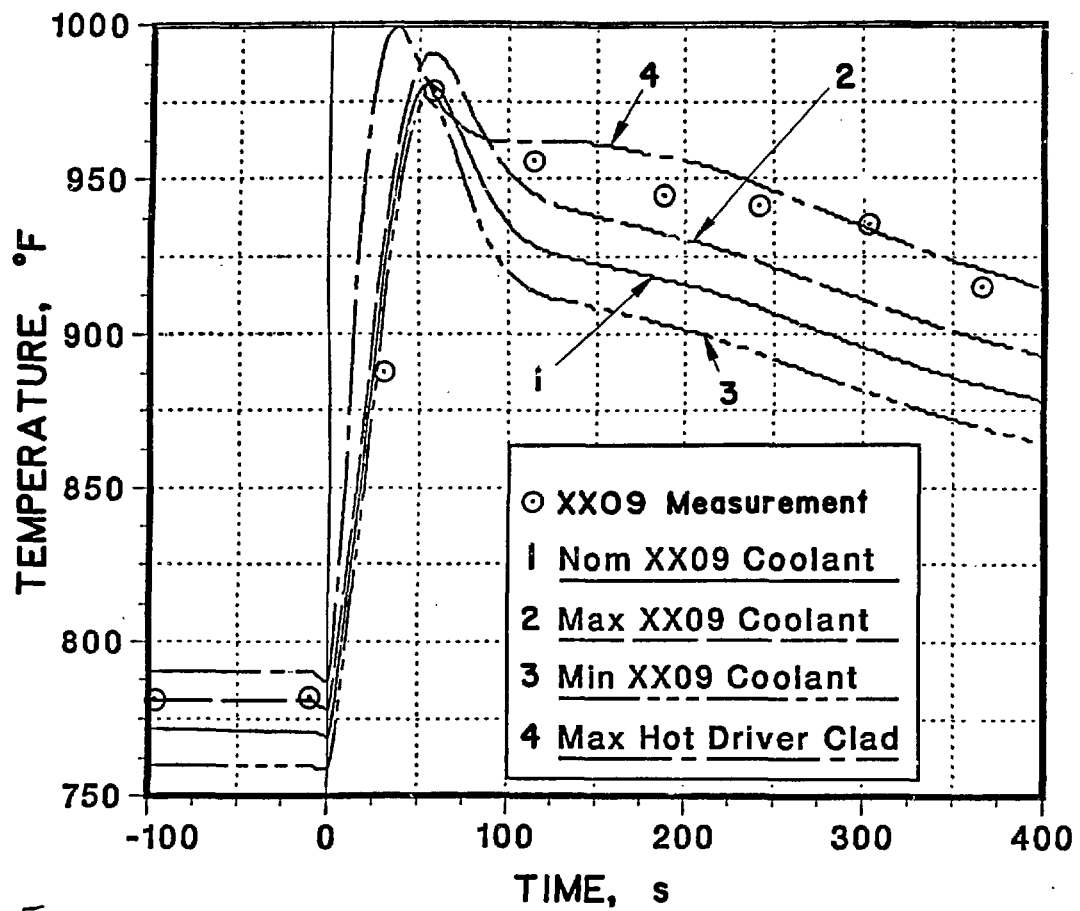


Fig. VI.11

Fig. 3. Predicted and Measured Top of Core Temperatures for the Transition to Natural Circulation from Shutdown Conditions (SHRT 2)

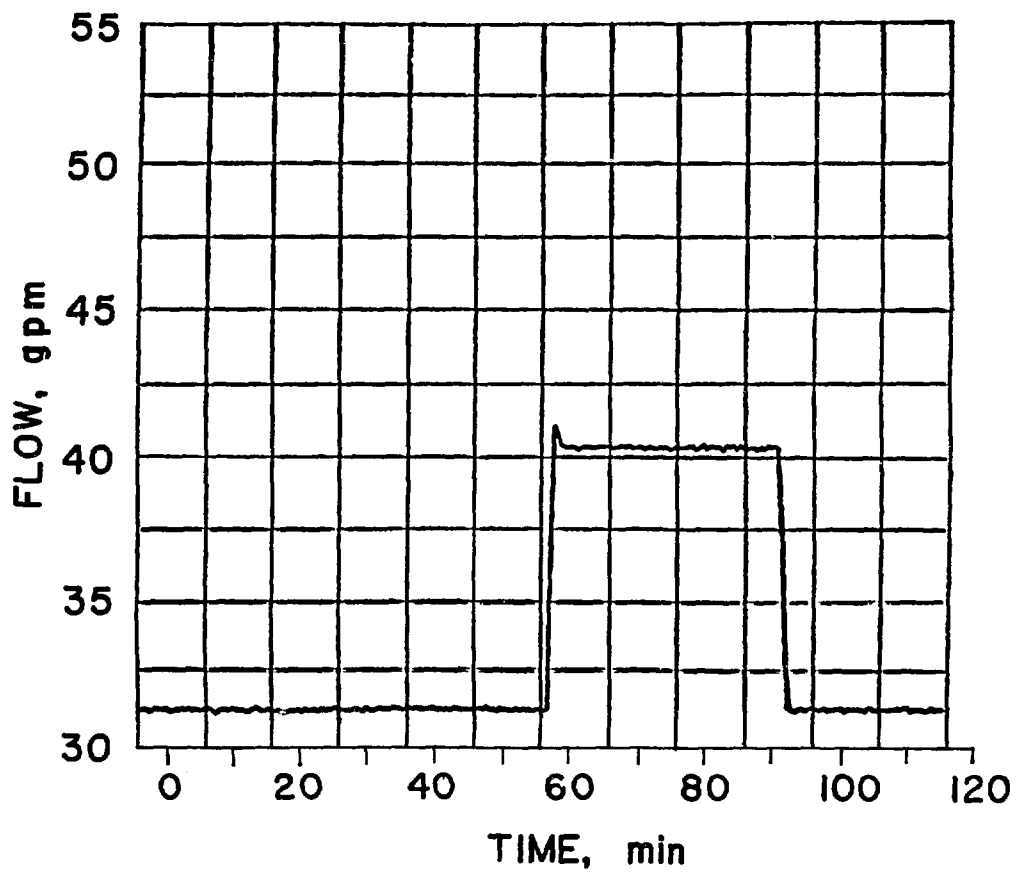


Fig. VI.12

Fig. 4. Flow Measured in the Instrumented Subassembly XX09 for the Flow Perturbation Test (SHRT 25)

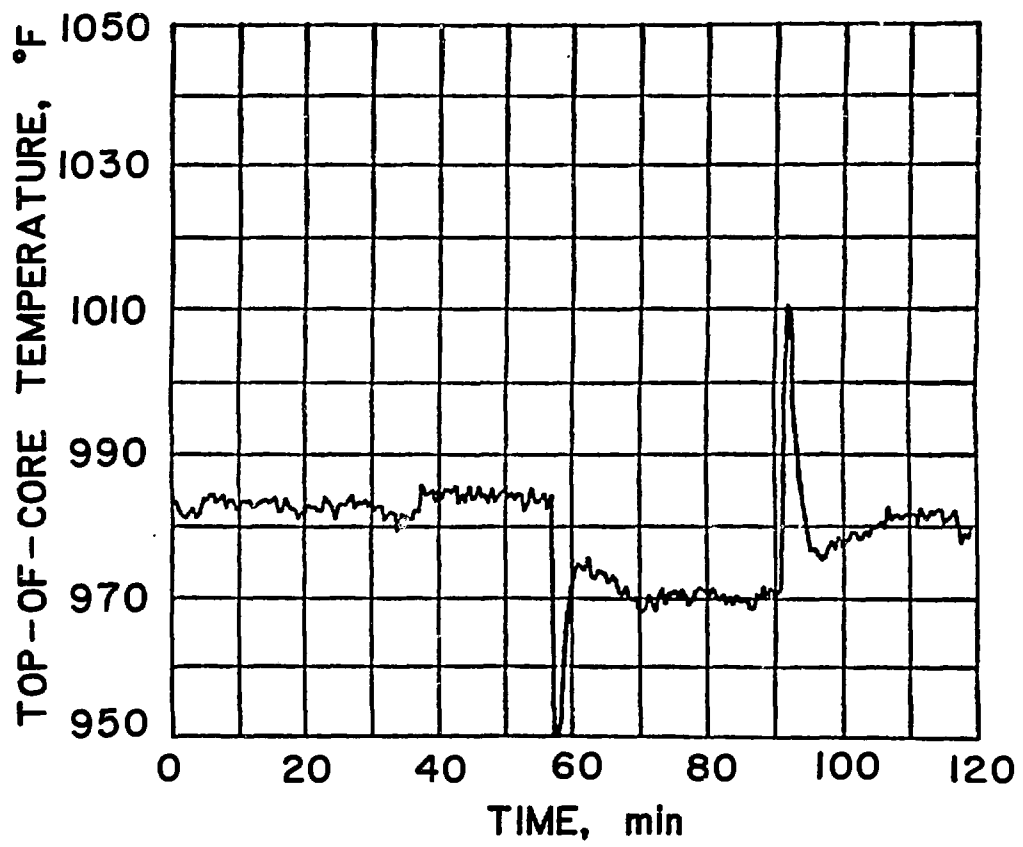


Fig. IV.13

Fig. 5. Top of Core Temperature Measured in XX09 During SHRT 25

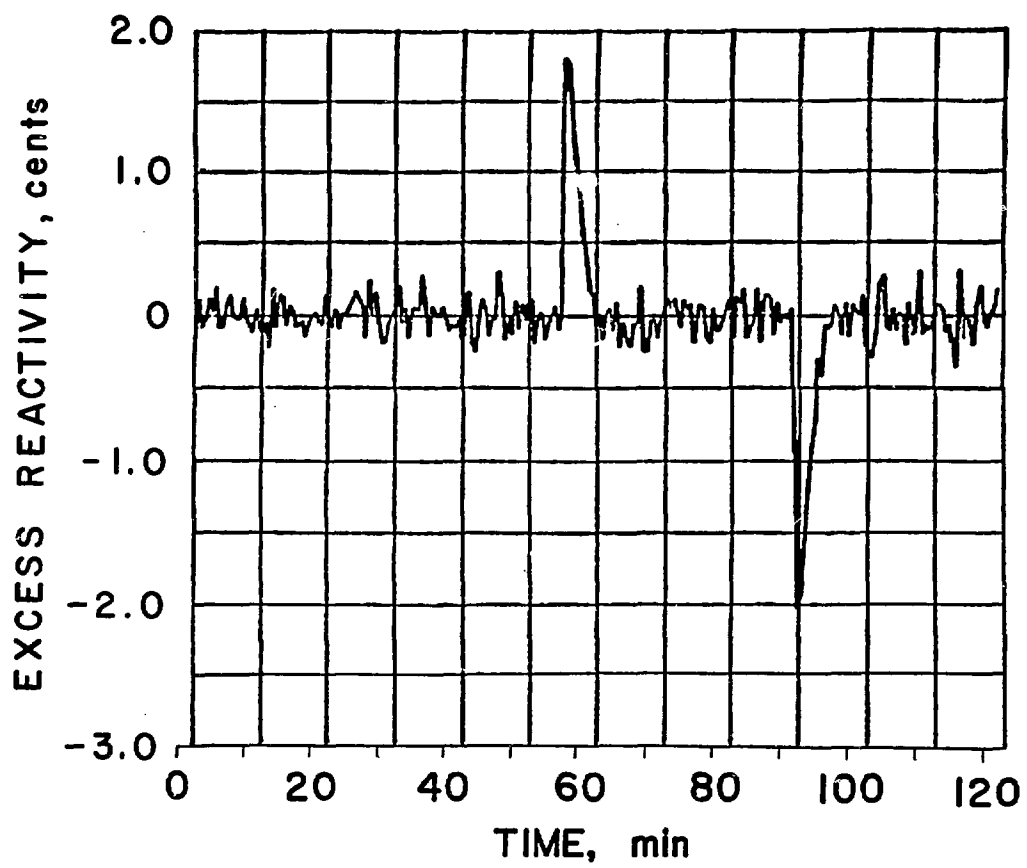


Fig. VI.14

Fig. 6. Excess Reactivity Calculated On-line During SHRT 25

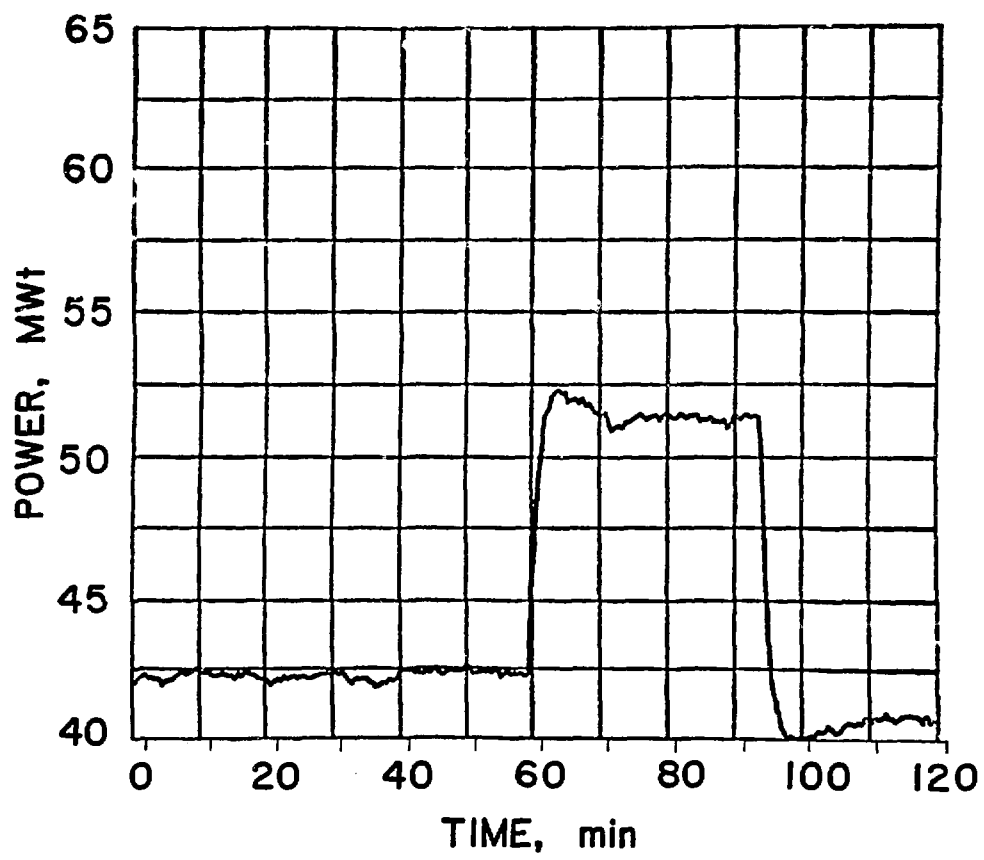


Fig. II.15

Fig. 7. Reactor Power Measured During SHRT 25

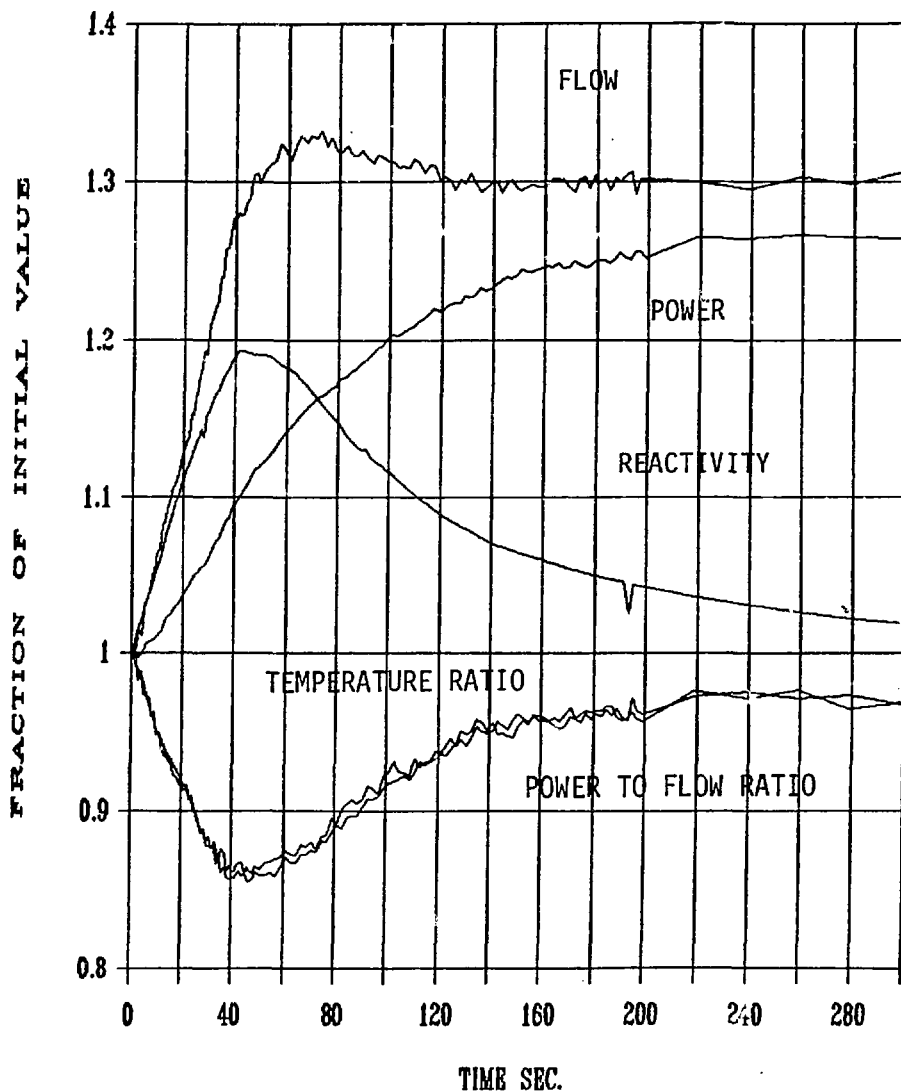


Fig. 8. Comparisons of Power, Flow, Temperature and Reactivity During SHRT 25

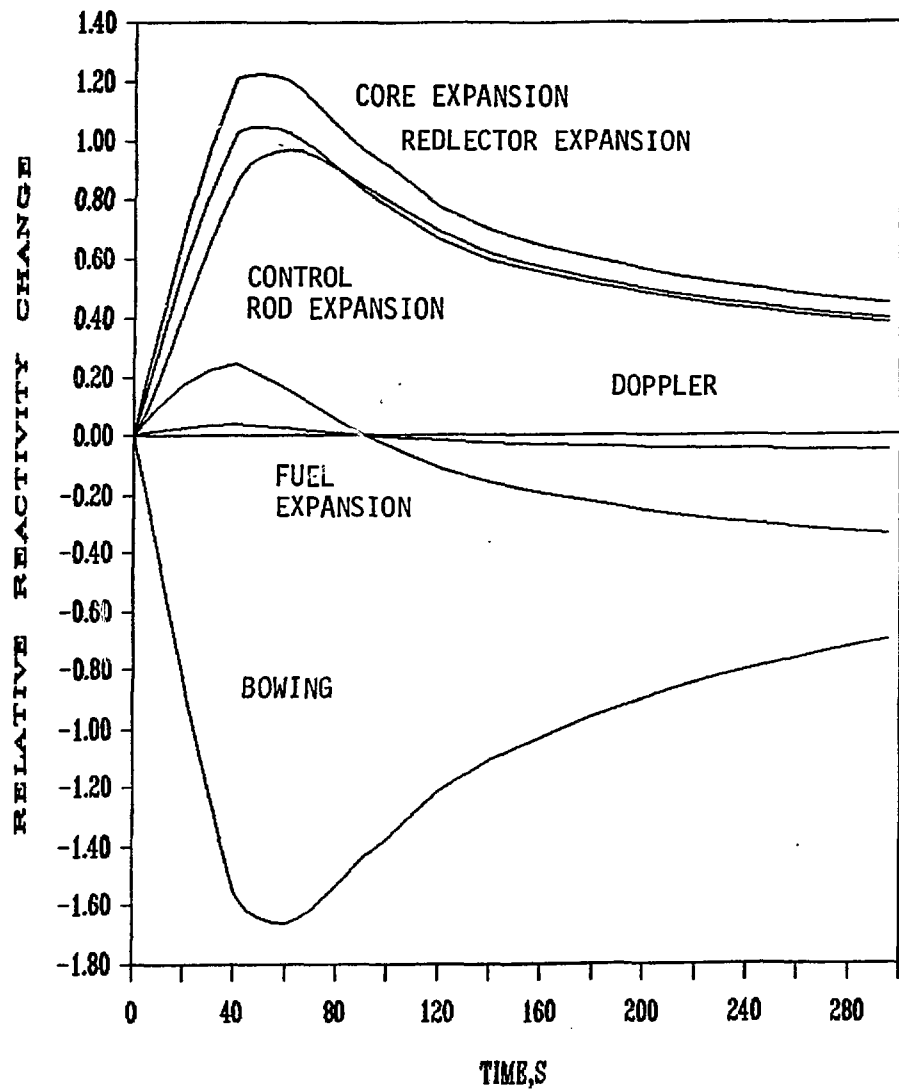


Fig. 9. Comparison of Reactor Feedback Changes for SHRT 25

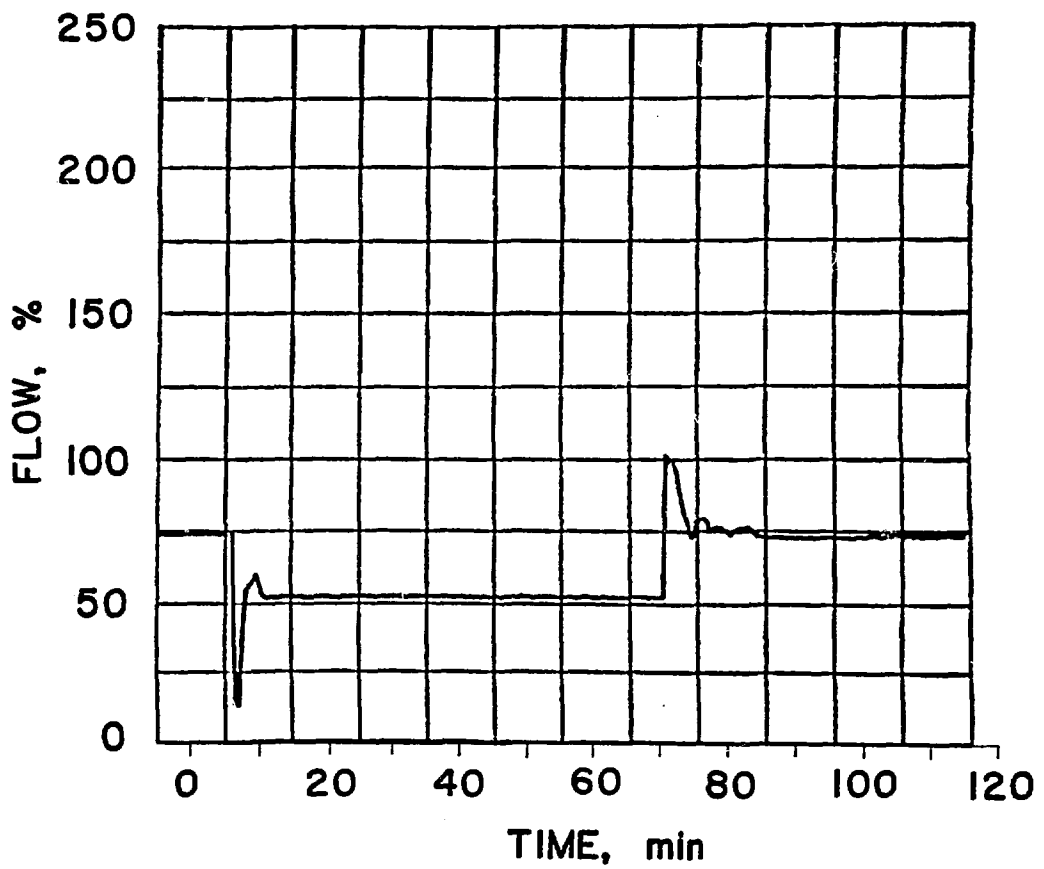


Fig. 10. Secondary Flow Measured During the Heat Sink Perturbation Test (SHRT 26)

11.5

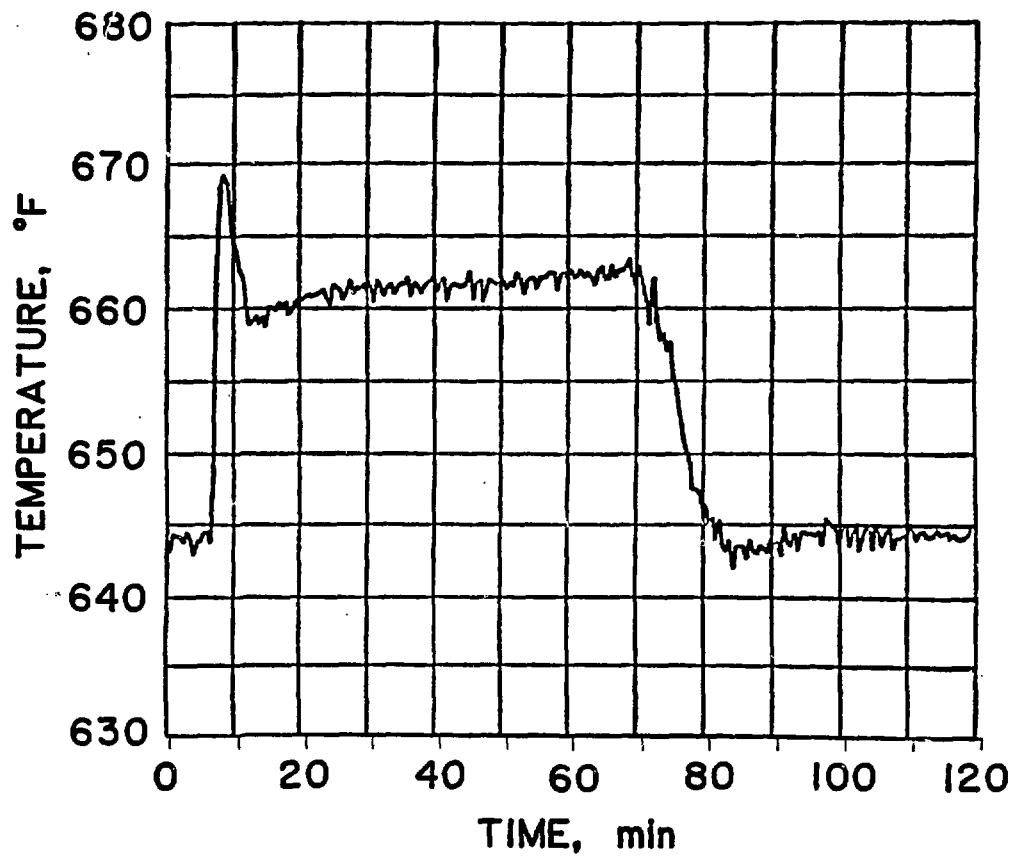


Fig. 11.17

Fig. 11. Reactor Inlet Temperature Measured in the Instrumented Subassembly XX09 During SHRT 26

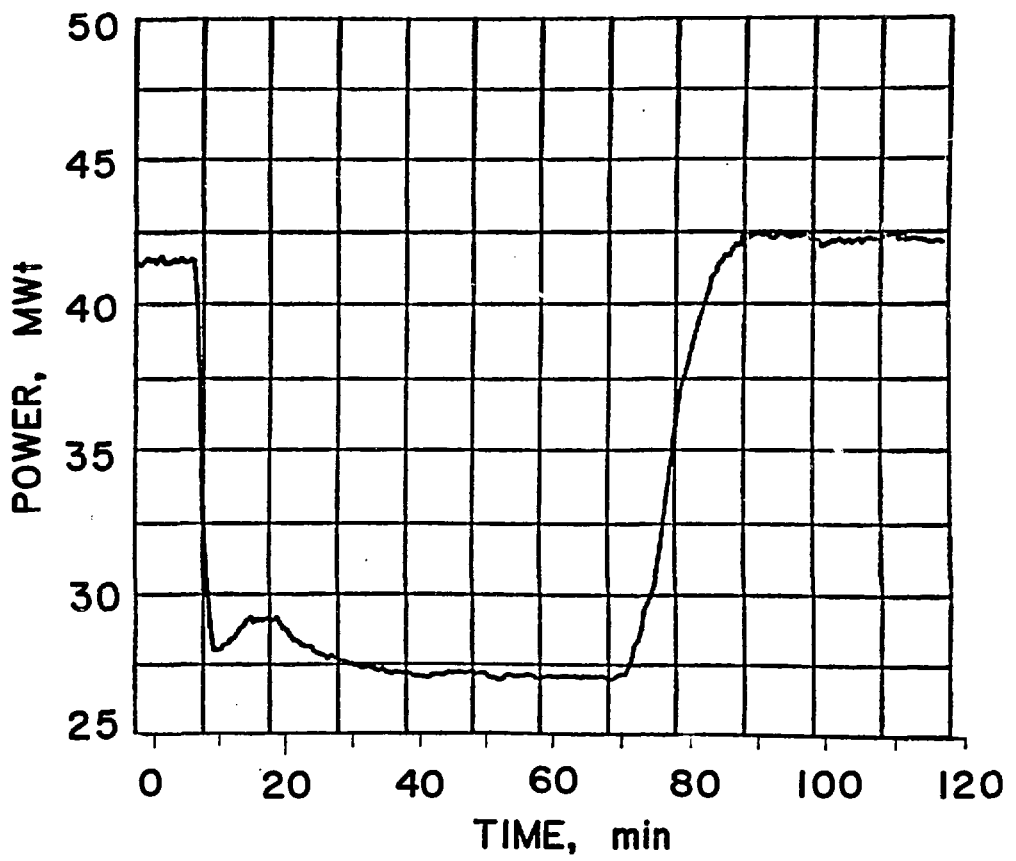


Fig. 12

Fig. 12. Reactor Power Measured During SHRT 26

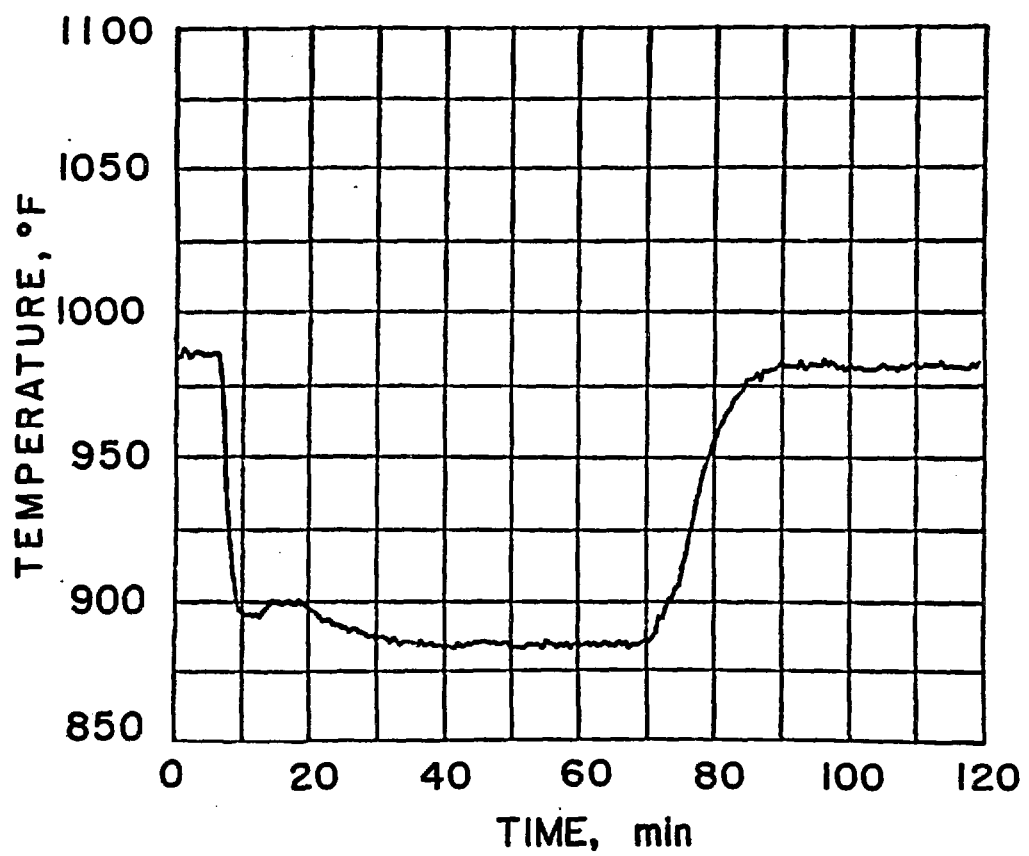


Fig. II.19

Fig. 13. Top of Core Temperature Measured in XX09 During SHRT 26